Single-Cysteine Substitution Mutants at Amino Acid Positions 55−75, the Sequence Connecting the Cytoplasmic Ends of Helices I and II in Rhodopsin: Reactivity of the Sulfhydryl Groups and Their Derivatives Identifies a Tertiary Structure that Changes upon Light-Activation[†,‡]

Judith Klein-Seetharaman,[§] John Hwa,[§] Kewen Cai,[§] Christian Altenbach,[||] Wayne L. Hubbell,[||] and H. Gobind Khorana*[,§]

Massachusetts Institute of Technology, Cambridge, MA 02139, and Jules Stein Eye Institute, UCLA, Los Angeles, CA 90095

Received January 4, 1999; Revised Manuscript Received April 8, 1999

ABSTRACT: Cysteines were introduced, one at a time, at amino acid positions 55−75 in the cytoplasmic region connecting helices I and II in rhodopsin. In each of the 21 cysteine mutants, the reactive native cysteine residues (C140 and C316) were replaced by serine. Except for N55C, all mutants formed rhodopsin-like chromophores and had normal photobleaching characteristics. The efficiency of G_T activation was reduced only for K66C, K67C, L68C, and P71C. The reactivity of the substituted cysteine in each mutant toward 4,4′-dithiodipyridine (4-PDS) was investigated in the dark. The mutants F56C to L59C and I75C were unreactive to 4-PDS under the conditions used, suggesting that they are embedded in the micelle or protein interior. The mutants V63C, H65C−T70C, and N73C reacted rapidly, while the remainder of the mutants reacted more slowly, and varied in reactivity with sequence position. For the mutants derivatized with 4-PDS, the rate of release of thiopyridone from the resulting thiopyridinyl-cysteine disulfide bond by dithiothreitol was investigated in the dark and in the light. Marked changes in the rates of thiopyridone release in the light were found at specific sites. Collectively, the data reveal tertiary interactions of the residues in the sequence investigated and demonstrate structural changes due to photoactivation.

Recent studies on structure and function in rhodopsin, the prototypic G-protein-coupled receptor, have provided insights into the mechanism of folding in vivo using mammalian cell lines. It has been concluded that the process of assembling the seven transmembrane (TM[1]) helices is coupled to the folding of the intradiscal region to form a tertiary structure (*2*−*8*). Furthermore, this structure changes upon illumination to a new structure that mediates protein−protein interactions required for visual transduction.

Multiple lines of evidence from previous work reveal the presence of a tertiary structure in the cytoplasmic region of rhodopsin. For example, in a mutant with a cysteine at position 65, a disulfide bond rapidly forms between C65 and the native C316, although these residues are at opposite ends of the primary sequence (Figure 1; ref *9*). Similarly, in double-cysteine mutants, a cysteine residue at 139 (in the cytoplasmic sequence connecting helices III−IV) readily forms a disulfide bond with another cysteine placed between amino acid positions 248 and 251 in the sequence connecting helices V and VI (*10*). These results suggest that the two cysteines are proximal, reflecting the tertiary structure.

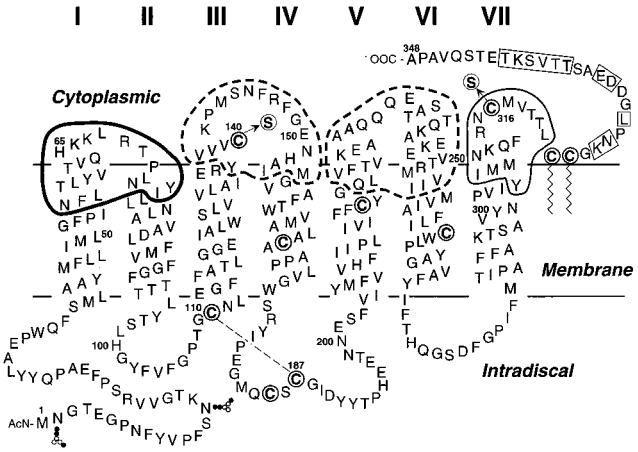

FIGURE 1: A secondary structural model of bovine rhodopsin showing the location of cysteine substitution sites studied in the present work, N55C to I75C (bold outline). Also indicated are sequences investigated in previous work (dashed outline) and those in accompanying papers (thin outline). Cysteines at positions 140 and 316 were replaced by serines (dotted circles) in all mutants.

Efforts to define the tertiary structures present in the cytoplasmic face of rhodopsin, both in the dark and light, continue. One general strategy has been that of cysteine scanning mutagenesis (*9*−*17*). The present paper describes

[†] Research reported here was supported by NIH Grants GM28289, EY11716 (H.G.K.), and EY05216 (W.L.H.) and the Jules Stein Professorship Endowment. J.K.-S. is the recipient of a Howard Hughes Medical Institute Predoctoral Fellowship. J.H. is the recipient of a Howard Hughes Medical Institute Postdoctoral Fellowship.

[‡] This is paper 32 in the series "Structure and Function in Rhodopsin". The preceding paper is Altenbach et al. (*1*).

* To whom correspondence should be addressed.

[§] Massachusetts Institute of Technology.

[||] Jules Stein Eye Institute, UCLA.

[1] Abbreviations: WT, wild type; 4-PDS, 4,4′-dithiodipyridine; 4-TP, 4-thiopyridone; DTT, dithiothreitol; DM, dodecylmaltoside; G_T, transducin; SDSL, site-directed spin labeling; TM, transmembrane; Meta II, Metarhodopsin II.

10.1021/bi990013t CCC: $18.00
Published on Web 06/02/1999

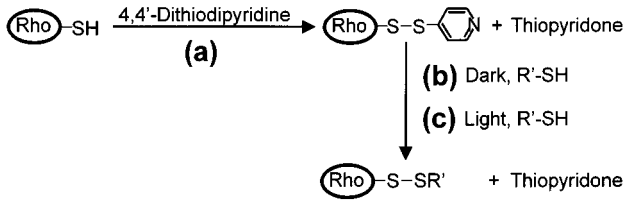

FIGURE 2: Reaction of (a) 4-PDS with rhodopsin cysteine mutants to form thiopyridinyl-cysteine derivatives and (b) thiopyridinyl-cysteine mutants with DTT in the dark and (c) after illumination.

cysteine scanning mutagenesis through the sequence 55−75 that encompasses residues between the cytoplasmic ends of helices I and II. Together with accompanying papers (*18*, *19*), the results reported herein bring to completion a series of experiments involving single-cysteine substitution mutagenesis for most of the cytoplasmic face of rhodopsin.

As reported here, the three types of experiments indicated in Figure 2 were carried out. In the first (Figure 2a), the rate of reaction of each cysteine mutant with 4-PDS to produce a thiopyridinyl-cysteine mixed disulfide was determined as a measure of the reactivity and solvent accessibility of the individual cysteines. In the second and third experiments (Figure 2, parts b and c), the rates of 4-TP formation from the mixed-disulfide product by DTT from the reaction in Figure 2a were determined in the dark and after photoactivation, respectively (Figure 2, parts b and c). The difference in these latter rates provides a measure of changes in accessibility and/or reactivity of the cysteine derivatives due to photoactivation. Presumably, changes in 4-TP release rates then reflect local conformational changes.

For reaction a in Figure 2, large differences in reactivity of the cysteine mutants toward 4-PDS were observed. Cysteines at positions 56−59 and 75 were totally unreactive to 4-PDS, suggesting that they were embedded in the micellar structure or the protein interior. The cysteines between 60 and 74 reacted with the reagent, but the rates varied widely with sequence position. This pattern of reactivity is consistent with a micelle−aqueous boundary near residues 60 and 74.

The rates of 4-TP release from the thiopyridinyl-cysteine disulfide bond (reaction b) by reaction with DTT varied over 4 orders of magnitude in the dark. Photoactivation of rhodopsin to produce Meta II caused dramatic changes in the rates of 4-TP release relative to the dark state, especially for sites near helix II. The differences in reactivity observed in the three sets of experiments are consistent with the presence of a tertiary structure that undergoes a change upon photoactivation of the receptor.

MATERIALS AND METHODS

Materials. All materials used were as described in an accompanying paper (*18*). The buffers used were the following: buffer A, 137 mM NaCl, 2.7 mM KCl, 1.8 mM KH_2PO_4, 10 mM Na_2HPO_4, pH 7.2; buffer B, buffer A plus 1% (wt/vol) DM; buffer C, buffer A plus 0.05% DM; buffer D, 5 mM 2-(*N*-morpholino)ethanesulfonic acid (MES), pH 6.0, 0.05% DM; buffer E, 2 mM NaH_2PO_4, pH 6.0, 0.05% DM.

Construction of Single-Cysteine Mutants. All mutants containing single cysteines in the sequence 55−75 were prepared from a "base" mutant of the synthetic bovine opsin gene in which the codons for the native cysteines C140 and C316 (TGC) were replaced by the serine codon (TCT) (*20*). The expression vector was pMT4 (*21*). The base mutant was prepared from the C140S mutant previously described (*21*) by replacing the *Mlu*I/*Not*I (nucleotides 758−1059) restriction fragment by the corresponding fragment containing the serine codon (*11*).

The mutants N55C, F56C, L57C, T58C, L59C, Y60C, V61C, T62C, V63C, Q64C, and K66C were prepared from the "base" mutant by fragment replacement mutagenesis. Synthetic oligonucleotides containing the cysteine codons corresponding to the restriction fragment *Bcl*I/*Hind*III (nucleotides 147−205) were used to replace the WT fragment. The mutant H65C has been described previously (*9*). For mutants R69C, T70C, P71C, L72C, N73C, Y74C, and I75C, DNA duplexes containing the cysteine codons (TGC) replaced the native restriction fragment *Hind*III/*Bgl*II (nucleotides 206−252).

PCR mutagenesis was used for preparation of the mutants K67C and L68C. The first step involved PCR reactions with the plasmid pMT4 containing the WT opsin gene as the template using primer 5′-GTCCAGCACAAG*TGC*CTTCG-CACACCG-3′ for mutant K67C and the primer 5′-CCAG-CACAAGAAG*TGC*CGCACACCGCTC-3′ for mutant L68C (the cysteine codon is in italics). The details of the PCR reaction have been described in an accompanying paper (*18*). The PCR products were digested to give the *Eco*RI/*Xho*I fragments (nucleotides 2−340) containing the cysteine codons, which were then subcloned into the large fragment *Xho*I/*Eco*RI (nucleotides 341−6182) of the base mutant. The DNA sequences of the fragments containing the mutated regions in all constructs were confirmed by the dideoxynucleotide sequencing method (*22*). Rhodopsin mutants were expressed and purified as described (*18*).

Determination of the Reactivity of the Cysteine Groups in Rhodopsin Mutants toward 4-PDS. The procedure for investigating the chemical reactivity of the sulfhydryl groups with 4-PDS was as reported in an accompanying paper (*18*) with the following minor modifications. 4-PDS in buffer E was added to the mutant samples in the same buffer such that the final solution contained 0.5 μM rhodopsin and 25 μM 4-PDS. The reaction was followed by the increase in absorbance at 323 nm, due to 4-TP release (Figure 2a), using the same concentration of 4-PDS without protein as a reference. Subtraction of the background contribution, the molar extinction coefficient of 4-TP at 323 nm, and calculation of the molar ratio of sulfhydryl groups per rhodopsin were all as previously described (*16*).

Modification of the Cysteine Mutants with 4-PDS and Rates of 4-TP Release with DTT. For preparative purposes, the reaction with 4-PDS to form the thiopyridinyl-cysteine mixed disulfides (Figure 2a) was performed while the mutants were bound to a 1D4-Sepharose matrix. After coupling the mutants to the 1D4-Sepharose matrix, the beads were washed with 50 bed volumes of buffer C and 50 bed volumes of buffer E. This was followed by the addition of 0.1 mM 4-PDS in buffer E and nutation in the dark for 3 h at room temperature or overnight at 4 °C. After being washed with 250 bed volumes of buffer E, the derivatized mutants were eluted with the nona-peptide epitope of the 1D4 antibody, as described (*23*).

The rates of 4-TP release from the thiopyridinyl derivatives with DTT were determined spectrophotometrically at 323

Table 1: Characterization of Single-Cysteine Substitution Mutants, F56C−I75C

mutant	UV/vis λ_{max} (nm)	absorbance A_{280}/A_{500}	meta II decay $T_{1/2}$ (min^{-1})
WT	500	1.6	11.8
F56C	498	1.7	9.3
L57C	499	1.8	10.0
T58C	499	1.7	9.8
L59C	502	1.6	10.6
Y60C	499	1.8	10.6
V61C	500	1.7	8.2
T62C	498	2.1	12.5
V63C	499	2.0	11.2
Q64C	499	2.0	11.2
H65C	499	1.7	9.2
K66C	499	1.9	10.0
K67C	499	1.8	11.0
L68C	499	1.8	12.3
R69C	499	1.8	13.1
T70C	498	2.1	7.3
P71C	499	1.9	7.9
L72C	499	1.9	11.7
N73C	498	1.8	11.4
Y74C	499	1.8	11.3
I75C	499	2.0	11.6

nm (Figure 2b). The thiopyridinyl derivatives were equilibrated at 4 °C in cuvettes for 30 min prior to the experiment. Ten microliters of a 3, 30, or 300 mM stock solution of DTT in buffer E was added to 290 μL of the modified rhodopsin mutant. The final concentrations were 5 μM rhodopsin and 0.1, 1, or 10 mM DTT.

In the reactions of cysteine mutants with 4-PDS, the concentration of the latter was chosen in 50-fold excess. Similarly, in the reactions of thiopyridinyl-cysteine mixed disulfides with DTT, the DTT concentration was in 200-fold excess at 0.1 mM DTT, 2000-fold at 1 mM, and 20000-fold at 10 mM DTT. Thus, both reactions followed pseudo-first-order kinetics, and the rate constants were calculated from monoexponential curve-fits (Sigmaplot) to the 323 nm absorbance data as a function of time.

RESULTS

Characterization of the Rhodopsin Cysteine Mutants, N55C−I75C. All cysteine mutants were expressed in COS cells and purified by immunoaffinity absorption as described in Methods. All mutants except for N55C formed a WT-like chromophore with λ_{max} at 498−502 nm. The spectral ratios (A_{280}/A_{500}) after elution from the 1D4-matrix at pH 7.2 (buffer C) were between 2.0 and 2.7, while elution at pH 6 (buffer E) gave ratios between 1.6 and 2.1 (Table 1). The mutant N55C formed chromophore poorly, and most of the protein was eluted only at pH 7.2 containing salt (buffer C). The reason for this remains to be determined. Upon illumination, all of the mutants formed the characteristic Meta II intermediate with half-lives similar to that of the WT (Table 1).

Rates of Reaction of the Sulfhydryl Groups in the Cysteine Mutants with 4-PDS (Figure 2a). Figure 3 shows representative data for the reaction of 4-PDS with N73C, Y74C, P71C, and I75C. The solid line in each case is the least-squares best fit of the data to a single exponential. From such fits, the pseudo-first-order rate constant for each reaction was determined. Table 2 gives the rate constants for the reactions

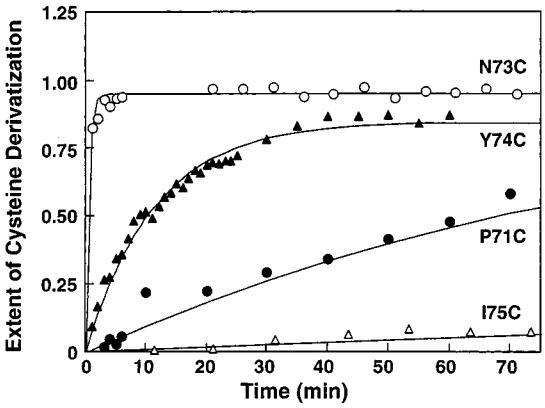

FIGURE 3: Reaction of SH groups for the indicated single-cysteine mutants with 4-PDS in the dark. The solid curves correspond to single-exponential fits.

Table 2: Reactivity of Mutants Y60C−I75C with 4-PDS

mutant	rate constant[a] (min^{-1})	mutant	rate constant[a] (min^{-1})
Y60C	0.24 ± 0.07	L68C	>1.4
V61C	0.006 ± 0.002	R69C	>1.4
T62C	0.015 ± 0.002	T70C	>1.4
V63C	>1.4[b]	P71C	0.0099 ± 0.0003
Q64C	0.39 ± 0.16	L72C	0.11 ± 0.01
H65C	>1.4	N73C	>1.4
K66C	>1.4	Y74C	0.11 ± 0.02
K67C	>1.4		

[a] Each rate constant was the average of at least three measurements. The error is the standard deviation. [b] For all ">1.4" values: the reaction was complete at the first time point taken (~1 min).

of all mutants as the average of three independent determinations. The mutants fell into four groups with respect to cysteine reactivity, illustrated by the four cases in Figure 3. One group, made up of V63C, H65C, K66C, K67C, L68C, R69C, T70C, and N73C, reacted so rapidly that the reactions were complete when the first spectrum was recorded (1 min). At the other extreme, F56C−L59C and I75C showed essentially no reaction with 4-PDS. The mutants V61C and P71C formed a group that reacted extremely slowly, while the remaining mutants, Y60C, T62C, Q64C, L72C, and Y74C, showed intermediate reactivities. For each reactive mutant, approximately one sulfhydryl group per mole of rhodopsin was modified at the end of the reaction.

Rates of 4-TP Release from the Thiopyridinyl-Cysteine Disulfide Bond in Derivatized Mutants (Figure 2b,c). Because of the wide variation in reactivity of the mixed disulfide bond in the thiopyridinyl-cysteine derivatives, it was necessary to use DTT at different concentrations (range from 0.1 to 10 mM) to obtain an accurate measure of 4-TP release rates. This was particularly important for the study of reactivity after illumination, because of the constraint imposed by the limited half-lives of the Meta II intermediates. All reactions were carried out at 4 °C where the Meta II half-life was 77 min.

Reduction Rates in the Dark State. Figure 4 shows the rates of reaction with DTT for all thiopyridinyl-cysteine mutants in the sequence 60−74 in the dark state (solid symbols) measured as 4-TP production. As indicated in the figure, the mutants fell into three groups on the basis of reactivity. One group, including H65C, K66C, K67C, L68C, T70C, and L72C, had derivatives of high reactivity, and the rates could be conveniently measured with 0.1 mM DTT

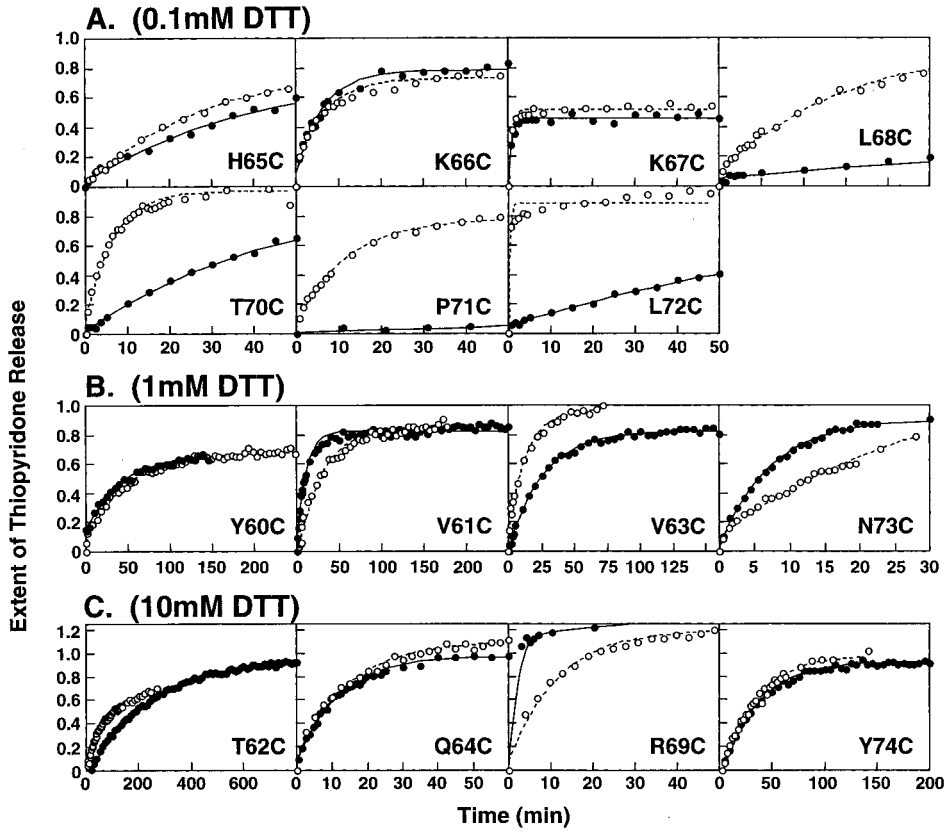

FIGURE 4: Reduction rates of the thiopyridinyl-cysteine derivatives of the mutants by DTT. Reactions were carried out at 4 °C in the dark (solid symbols) and after illumination (open symbols). Depending upon the reactivities of the thiopyridinyl-cysteine disulfide bond, the reactions were studied at one of three concentrations of DTT: 0.1 mM (A), 1 mM (B), and 10 mM (C). The concentration of the rhodopsin mutants was 0.5 μM in every case.

(Figure 4a). Another group, consisting of Y60C, V61C, V63C, and N73C, had derivatives of intermediate reactivity whose reduction rates could be conveniently measured at 1 mM DTT (Figure 4b). Finally, T62C, Q64C, and Y74C had derivatives of low reactivity, and 10 mM DTT was required for the measurement of the rates of reduction (Figure 4c). In the case of R69C (Figure 4c), P71C, L68C, and L72C (Figure 4a), the grouping was primarily based on the reactivity in the light (see below). Table 3 gives the rate constants divided by the DTT concentrations used in the measurement.

The rate constants of the mutants in the highly reactive group (0.1 mM DTT) and the slowest reacting group (10 mM DTT) differed by up to 4 orders of magnitude (Table 3). Thus, at the lowest DTT concentration (0.1 mM), the K67C derivative released 4-TP effectively instantaneously with an estimated maximum half-life of $T_{1/2} \leq 1$ min. Thus the minimum rate constant would be 1.4 min^{-1} (psuedo-first-order) or 14 min^{-1} [mM DTT]$^{-1}$ (true second-order). The derivative of mutant T62C was the slowest, showing at 10 mM DTT a reaction rate constant of 0.0047 ± 0.0001 min^{-1} or 0.00047 min^{-1} [mMD TT]$^{-1}$.

4-TP Release Rates after Illumination. After illumination, the thiopyridinyl-cysteine derivatives of all mutants except K66C and Y74C showed changes in rates of 4-TP release relative to the dark state (Figure 4, open symbols; Table 3). The changes were most dramatic near helix II, namely at L68C to N73C. In particular, the derivative of P71C reacted 340 times faster and that of L72C at least 74 times faster in the light than in the dark. In contrast, the derivatives of R69C and N73C both reacted slower in the light than in the dark. Figure 5 shows a graphical representation of the logarithm of the ratio of the rates in the light and dark for each mutant. For derivatives of mutants K67C and T62C, accurate rate determinations in the light could not be carried out at any of the three DTT concentrations. The K67C derivative reacted effectively instantly both in the dark and in the light. For the T62C derivative, the reaction after illumination was too slow to be measured reliably within the Meta II half-life of 77 min at 4 °C, even at 10 mM DTT.

Table 3: Rate Constants for Reduction of Thiopyridinyl-Cysteine Derivatives by DTT[a]

mutant	dark	light
Y60C	0.0251 ± 0.0003[b]	0.0319 ± 0.0005[b]
V61C	0.084 ± 0.008[b]	0.0357 ± 0.0006[b]
T62C	0.00047 ± 0.00001[c]	0.0015 ± 0.0001[c]
V63C	0.036 ± 0.002[b]	0.06 ± 0.01[b]
Q64C	0.0083 ± 0.0001[c]	0.0065 ± 0.0004[c]
H65C	0.24 ± 0.07[d]	0.42 ± 0.05[d]
K66C	1.5 ± 0.1[d]	1.51 ± 0.07[d]
K67C	>14[d]	>14[d]
L68C	0.034 ± 0.004[d]	0.42 ± 0.01[d]
R69C	>0.14[c]	0.00869 ± 0.0003[c]
T70C	0.25 ± 0.03[d]	1.4 ± 0.1[d]
P71C	0.00246 ± 0.00009[c]	0.84 ± 0.02[d]
L72C	0.0925 ± 0.0001[d]	>14[d]
N73C	0.12 ± 0.02[b]	0.031 ± 0.004[b]
Y74K	0.00279 ± 0.00006[c]	0.00301 ± 0.00007[c]

[a] The rate constants are the true second-order rate constants, min^{-1} $[mM]^{-1}$, calculated by dividing the experimentally determined pseudo-first-order values by the DTT concentrations. [b] Measured at 1 mM DTT. [c] Measured at 10 mM DTT. [d] Measured at 0.1 mM DTT.

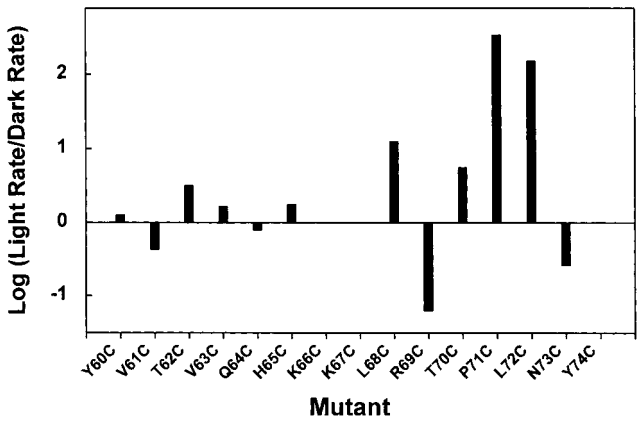

FIGURE 5: The effect of photoactivation on the reduction rate of thiopyridinyl-cysteine derivatives by DTT. The data from Table 3 are plotted as the logarithm of the ratio of the rate constants (light/dark) for each mutant.

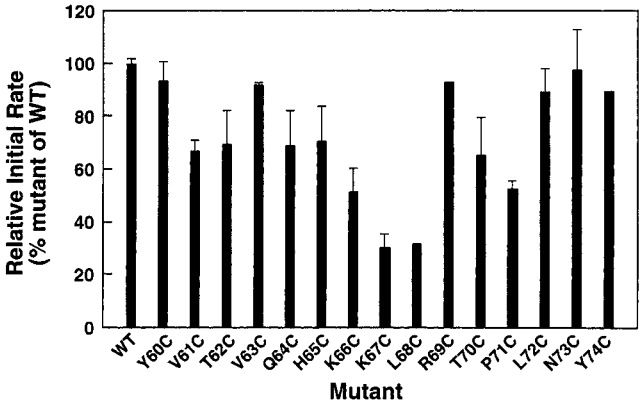

FIGURE 6: Comparison of the initial rates for activation of G_T by the cysteine substitution mutants. The initial rates of fluorescence increase for each mutant were calculated from fluorescence data as described in ref *18*. Each rate is the average of at least two measurements.

G_T Activation. The ability of the single-cysteine mutants to activate G_T was monitored by the fluorescence increase assay, which determines the rate of formation of the G_T−GTPγS complex. The initial rates of complex formation for each mutant determined from this assay are compared in Figure 6. Most mutants showed rates of activation that were similar to that of WT rhodopsin. The mutants K67C and L68C showed decreases in G_T activation to about 30% of WT, while K66C and P71C showed decreases to about 50%. Thus, the effects on G_T activation were not remarkable compared to observations in other cytoplasmic sequences (*18*).

DISCUSSION

Reactivity of the Sulfhydryl Groups in the Cysteine Mutants in the Dark. The reaction kinetics of cysteine residues in rhodopsin with 4-PDS is determined, in part, by sulfhydryl solvent accessibility, properties of the local environment in the protein, and the polarity of the surrounding medium. While kinetic data alone cannot distinguish between the various effects, site-specific differences in reaction rates are likely to be dominated by the accessibility of the sulfhydryl group to the reagent and the state of ionization of the thiol group. For a cysteine residue on rhodopsin facing the micelle interior, the rate of reaction with 4-PDS is expected to be slow due to suppressed ionization of the thiol and the limited solubility of the polar 4-PDS molecule. For cysteine residues located in extramembranous sequences, the reaction rate is expected to vary primarily according to the degree of solvent accessibility, with minor electrostatic effects on the degree of sulfhydryl ionization. The reagent 4-PDS is particularly useful as a probe of reactivity in membrane proteins because it is electrically neutral and has no direct electrostatic interactions with the environment that would alter the local concentration or limit membrane permeability (*24*, *25*). Sequence-specific sulfhydryl reactivity with 4-PDS should then be a useful probe of local structure in rhodopsin, just as other reagents have found use in exploring specific structural features in other membrane proteins (*26*).

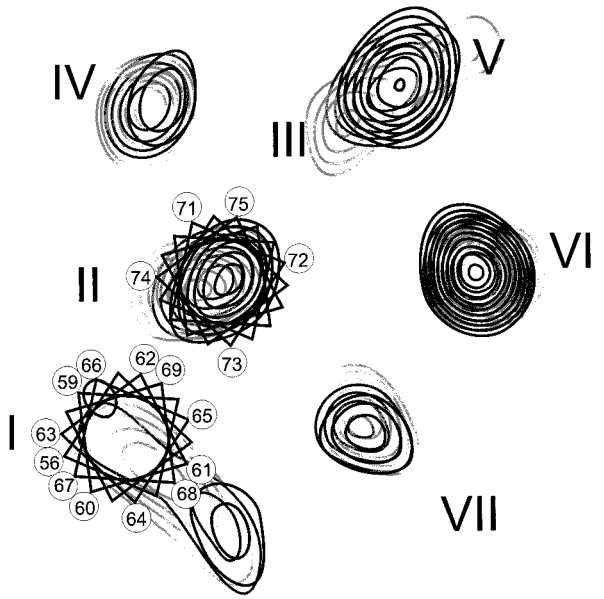

FIGURE 7: Helical wheel representation of the cytoplasmic ends of helices I and II of rhodopsin superimposed on the arrangement of the 7-transmembrane helical bundle based on cryo-electron microscopy studies (*27*). The electron density contour sections at 13, 15, and 17 Å (gray to black) from the center of the membrane are shown. The contour sections were from a three-dimensional map at an effective resolution of 7.5 Å in the membrane plane and 16.5 Å normal to the plane and were kindly provided by G. F. X. Schertler (personal communication). Residue positions are mapped onto the electron contour sections on the basis of SDSL studies (*28*).

In the paragraphs below, the reactivity of cysteine residues in the sequence 56−75 toward 4-PDS and the reactivity of their thiopyridinyl-cysteine derivatives in dark and light are discussed with respect to a current model of the rhodopsin structure. This model is based in part on the low-resolution 3-dimensional electron density map for rhodopsin determined by Schertler and co-workers from cryoelectron microscopy (*27*). The major features of the electron density map correspond to the TM helical segments, and little density is associated with the extramembranous segments connecting the helices at the cytoplasmic surface. On the other hand, previous SDSL studies have identified specific structures in the sequences connecting helices II−III and helices V−VI (*13*, *15*). In an accompanying paper, SDSL studies are reported that indicate that residues 56−63 and 72−75 are in a helical configuration corresponding to helices I and II and their extensions into the aqueous phase, respectively (*28*). Figure 7 shows a superposition of electron density contours

taken at sections 13, 15, and 17 Å from the center of the membrane. Also shown is the mapping of the helical residues in the sequence 56−75 as suggested by the SDSL studies (*28*). The 13 Å contour corresponds approximately to the location of the membrane−aqueous interface (*29*).

Residues F56C−L59C at the end of helix I and I75C in helix II showed no reaction with 4-PDS, while all residues from Y60C−Y74C showed measurable reactivity. These results suggest that the reactive residues Y60C−Y74C are exposed to the reagent. The other residues are likely to be sequestered in either the micelle or protein interior, where they would be unreactive for the reasons discussed above. This reactivity pattern further suggests that the rhodopsin polypeptide crosses the micelle−water interface somewhere in the neighborhood of residue Y60C and again near Y74C, marking the cytoplasmic terminations of TM helices I and II, respectively. However, the location of each crossing point is uncertain to within a turn of the helix (±3−4 residues), because the lack of reactivity alone cannot distinguish whether the residue is facing the micelle interior or the protein interior.

Residues within the sequence 60−74 showed wide variations in reactivity with 4-PDS. In the segment presumed to cross the micelle interior−aqueous interface, residues Y60C and V63C reacted very rapidly, while T62C and V61C reacted slowly with 4-PDS. This is consistent with the orientation of these residues determined from SDSL, where Y60C and V63C are facing the outside of the helical bundle and V61C and T62C are facing the protein interior (Figure 7). Residues H65C to T70C all reacted very rapidly with 4-PDS. This result supports the conclusion that the sequence 64−70 is water-solvated as derived from accessibility measurements of nitroxide spin labels at these positions (*28*).

Reactivity of Thiopyridine-Cysteine Mutants with DTT in the Dark. The reactivity of the disulfide bond in the thiopyridinyl-cysteine derivatives of the mutants as measured by 4-TP release varied over 4 orders of magnitude. The most reactive was the K67C derivative, suggesting that this residue is the most exposed or located in a unique chemical environment. Consistent with this finding is the very pronounced peak in mobility and solvent accessibility for a spin-label side chain at this position (*28*).

In general, the reactivity of the thiopyridinyl-derivatives with DTT roughly coincides with the reactivity of the free sulfhydryl groups toward 4-PDS, discussed above. For example, the mutants whose cysteines reacted rapidly with 4-PDS are also those whose derivatives react readily in the presence of 0.1 mM DTT. Similarly, P71C and T62C reacted very slowly with 4-PDS, and the corresponding thiopyridinyl-cysteine derivative reacted slowly with DTT. However, differences were found. For example, V63C reacted essentially instantaneously with 4-PDS, but its thiopyridinyl-derivative, as measured at 1 mM DTT concentration, reacted at a relatively slow rate compared to the other mutants (Table 3, Figure 4b). It is not surprising that such differences exist, because the reactions of the two reagents involve different steric requirements. In fact, this result emphasizes the fact that accessibility mapping of cysteine residues by reactivity may give different results for different reagents. However, changes in reactivity for a given reagent should be a reliable method for detecting local changes in structure.

Reactivity of Thiopyridinyl-Cysteine Mutants with DTT in the Light. The rate constants for 4-TP release from thiopyridinyl-cysteine mutants by DTT in the light and dark were up to 340-fold different. As seen in Figure 5, the differences were most pronounced in helix II and nearby residues (residues L68C−N73C), while very small or no changes were found in and around helix I (residues Y60C−K66C). Similarly, light-induced changes in the EPR spectra of spin labels are most prominent at residues near helix II (*28*).

The derivatives of L68C and T70C−L72C showed an increase in reactivity, in contrast to those of R69C and N73C, which showed decreased reactivity in the light. This suggests that R69C and N73C may be in proximity and experience similar changes upon light-activation. Indeed, this conclusion agrees well with the residue mapping shown in Figure 7 that places residues R69C and N73C close to each other. The thiopyridinyl-cysteine derivative of Y74C shows no change in reactivity with DTT upon photoactivation to the Meta II state, consistent with a placement of this residue toward the outside of the bundle with minimum interaction with other helices (Figure 7).

The largest changes in reduction rate due to photoactivation were observed with the derivatives of P71C and L72C. In the model of Figure 7, P71C and L72C point toward the interior of the helical bundle, in particular toward helix III. An increasing number of reports have identified helix III as one of the main players in the activation mechanism of rhodopsin (*13*, *30*, *31*). The results obtained from the changes in reactivities of the P71C and L72C derivatives presented here strongly support this conclusion. Indeed, in the helix packing model of Baldwin (*29*), residues P71C and L72C directly face E134 and R135. These two residues are part of the (D/E)RY sequence that is conserved throughout the entire family of G-protein-coupled receptors, and this region is believed to be involved in the activation of G_T.

G_T Activation by the Cysteine Mutants. The effects of cysteine replacements on G_T activation ability were relatively small. The majority of the mutants activated G_T in a WT-like manner, while K66C, K67C, L68C, and P71C showed 50−70% decrease in G_T activation. Previously, mutants at positions T58 and T70/P71 were found to affect G_T activation (32). Mutations L72A and N73A had only a small effect while mutants T62A/V63A/Q64, H65Y, K66A/K67A, L68A/R69A/T70A, and P71A were found to activate G_T in a WT-like manner (*33*). In a peptide inhibition study, the peptide 61−75, corresponding to the I−II interhelical sequence at the cytoplasmic face, did not compete with Meta II for binding to G_T. In contrast, peptides corresponding to sequences in the interhelical segment between helices III−IV and V−VI, and the sequence adjoining the palmitoyl groups (*34*), effectively competed with Meta II for binding of G_T. The lack of peptide inhibition and the overall minor effect of point mutations in this region suggests that the residues connecting helices I and II are not involved directly in recognition by G_T.

In summary, the pattern of reactivity of the cysteine substitution mutants with 4-PDS in the sequence 55−75 reflects the tertiary fold of rhodopsin around this I−II interhelical segment. A similar pattern, with some differences, is noted in the rate of reaction of DTT with thiopyridinyl-cysteine derivatives of the same mutants. The large changes in the latter rates around helix II upon

photoactivation reveals a structure rearrangement in the molecule. Finally, the relatively small effects of single-cysteine replacements throughout the sequence support the earlier conclusion that the I−II interhelical segment plays a lesser role in the interaction with G_T compared to the other cytoplasmic segments.

REFERENCES

1. Altenbach, C., Cai, K., Khorana, H. G., and Hubbell, W. L. (1999) *Biochemistry 38*, 7931−7937.
2. Doi, T., Molday, R. S., and Khorana, H. G. (1990) *Proc. Natl. Acad. Sci. U.S.A. 87*, 4991−4995.
3. Ridge, K. D., Lu, Z., Liu, X., and Khorana, H. G. (1995) *Biochemistry 34*, 3261−3267.
4. Garriga, P., Liu, X., and Khorana, H. G. (1996) *Proc. Natl Acad. Sci. U.S.A. 93*, 4560−4564.
5. Liu, X., Garriga, P., and Khorana, H. G. (1996) *Proc. Natl. Acad. Sci. U.S.A. 93*, 4554−4559.
6. Hwa, J., Garriga, P., Liu, X., and Khorana, H. G. (1997) *Proc. Natl. Acad. Sci. U.S.A. 94*, 10571−10576.
7. Reeves, P., Hwa, J., and Khorana, H. G. (1999) *Proc. Natl. Acad. Sci. U.S.A. 96*, 1927−1931.
8. Hwa, J., Reeves, P., Klein-Seetharaman, J., Davidson, F., and Khorana, H. G. (1999*) Proc. Natl. Acad. Sci. U.S.A. 96*, 1932−1935.
9. Yang, K., Farrens, D. L., Altenbach, C., Farahbakhsh, Z. T., Hubbell, W. L., and Khorana, H. G. (1996) *Biochemistry 35*, 14040−14046.
10. Farrens, D. L., Altenbach, C., Yang, K., Hubbell, W. L., and Khorana, H. G. (1996) *Science 274*, 768−770.
11. Resek, J. F., Farahbakhsh, Z. T., Hubbell, W. L., and Khorana, H. G. (1993) *Biochemistry 32*, 12025−12032.
12. Ridge, K. D., Zhang, C., and Khorana, H. G. (1995) *Biochemistry 34*, 8804−8811.
13. Farahbakhsh, Z. T., Ridge, K. D., Khorana, H. G., and Hubbell, W. L. (1995) *Biochemistry 34*, 8812−8819.
14. Yang, K., Farrens, D. L., Hubbell, W. L., and Khorana, H. G. (1996) *Biochemistry 35*, 12464−12469.
15. Altenbach, C., Yang, K., Farrens, D. L., Farahbakhsh, Z. T., Khorana, H. G., and Hubbell, W. L. (1996) *Biochemistry 35*, 12470−12478.
16. Cai, K., Langen, R., Hubbell, W. L., and Khorana, H. G. (1997) *Proc. Natl. Acad. Sci. U.S.A. 94*, 14267−14272.
17. Kim, J.-M., Altenbach, C., Thurmond, R. L., Khorana, H. G., and Hubbell, W. L. (1997) *Proc. Natl. Acad. Sci. U.S.A. 94*, 14273−14278.
18. Cai, K., Klein-Seetharaman, J., Farrens, D., Zhang, C., Altenbach, C., Hubbell, W. L., and Khorana, H. G. (1999) *Biochemistry 38*, 7925−7930.
19. Langen, R., Cai, K., Altenbach, C., Khorana, H. G., and Hubbell, W. L. (1999) *Biochemistry 38*, 7918−7924.
20. Ferretti, L., Karnik, S. S., Khorana, H. G., Nassal, M., and Oprian, D. D. (1986) *Proc. Natl. Acad. Sci. U.S.A. 83*, 599−603.
21. Franke, R. R., Sakmar, T. P., Oprian, D. D., and Khorana, H. G. (1988) *J. Biol. Chem. 263*, 2119−2122.
22. Sanger, F., Nicklen, S., and Coulson, A. R. (1977) *Proc. Natl. Acad. Sci. U.S.A. 74*, 5463−5467.
23. Oprian, D. D., Molday, R. S., Kaufman, R. J., and Khorana, H. G. (1987) *Proc. Natl. Acad. Sci. U.S.A. 84*, 8874−8878.
24. Grassetti, D. R., and Murray, J. F., Jr. (1967) *Arch. Biophys. 119*, 41−49.
25. Chen, Y. S., and Hubbell, W. L. (1978) *Membr. Biochem. 1*, 107−130.
26. Javitch, J. A., Li, Z., Kaback, H. R., and Karlin, A. (1994) *Proc. Natl. Acad. Sci. U.S.A. 91*, 10355−10359.
27. Unger, V. M., Hargrave, P. A., Baldwin, J. M., and Schertler, G. F. X. (1997) *Nature 389*, 203−206.
28. Altenbach, C., Klein-Seetharaman, J., Hwa, J., Khorana, H. G., and Hubbell, W. L. (1999) *Biochemistry 38*, 7945−7949.
29. Baldwin, J. M., Schertler, G. F. X., and Unger, V. M. (1997) *J. Mol. Biol. 272*, 144−164.
30. Farabakhsh, Z., Hideg, K., and Hubbell, W. L. (1993) *Science 262*, 1416−1419.
31. Sheikh, S. P., Zvyaga, T. A., Lichtarge, O., Sakmar, T. P., and Bourne, H. R. (1996) *Nature 383*, 347−350.
32. Min, K. C., Zvyaga, T. A., Cypess, A. M., and Sakmar, T. P. (1993) *J. Biol. Chem. 268*, 9400−9404.
33. Shi, W., Osawa, S., Dickerson, C. D., and Weiss, E. R. (1995) *J. Biol. Chem. 270*, 2112−2119.
34. König, B., Arendt, A., McDowell, J. H., Kahlert, M., Hargrave, P. A., and Hofmann, K. P. (1989) *Proc. Natl. Acad. Sci. U.S.A. 86*, 6878−6882.

BI990013T